BOLETÍN DE LA SOCIEDAD ESPAÑOLA DE CERÁMICA Y VIDRIO XXX (2024) XXX–XXX

BOLETIN DE LA SOCIEDAD ESPAÑOLA DE
Cerámica y Vidrio
www.elsevier.es/bsecv

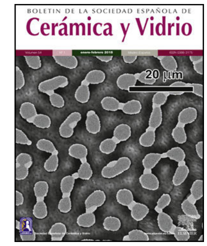

Original

Low-temperature sintering of ceramic bricks from clay, waste glass and sand

M. Flores Nicolás [a,*], M.M. Chávez Cano [a], M. Vlasova [b], T. Pi Puig [c]

[a] Instituto de Ingeniería, Universidad Nacional Autónoma de México UNAM, Circuito Escolar s/n, Ciudad Universitaria, Alcaldía Coyoacán, C.P. 04510, CDMX, Mexico
[b] Centro de Investigación en Ingeniería y Ciencias Aplicadas, Universidad Autónoma del Estado de Morelos (CIICAp-UAEMor), Av. Universidad 1001, Col. Chamilpa, Cuernavaca, Morelos, C.P. 62209, Mexico
[c] Instituto de Geología – LANGEM, Universidad Nacional Autónoma de México UNAM, Cd. Universitaria, Circuito de la Investigación Científica, Alcaldía Coyoacán, C.P. 04510, CDMX, Mexico

ARTICLE INFO

Article history:
Received 29 June 2023
Accepted 11 June 2024
Available online xxx

Keywords:
Clay
Waste glass
Sand
Mechanical properties of ceramic bricks
Plastic molding

ABSTRACT

In the present work, bricks were made on a real 1:1 scale for the construction of housing. For the preparation of the mixtures, raw materials such as clay, sand and glass obtained from the recycling of brown beer containers were used, applying the method plastic molding for the preparation of the semi-products. It has been established that the addition of sand containing a small amount of montmorillonite to such clay enabled to realization of plastic molding. The incorporation of glass into the clay provided to substantially reduce the sintering time of the bricks up to 8 h and to vary their strength properties. Sintering was carried out at 800 °C in an air atmosphere. The results of X-ray diffraction (XRD), X-ray fluorescence (XRF) and field emission scanning electron microscopy (FESEM) and EDS microanalysis have shown that the raw materials and ceramic bricks contains quartz and feldspars. Low-temperature sintering has made it possible to obtain high-quality, high-strength building bricks in accordance with standards.

Sinterización a baja temperatura de ladrillos cerámicos a partir de arcilla, residuos de vidrio y arena

Palabras clave:
Arcilla
Residuos de vidrio
Arena
Propiedades mecánicas de los ladrillos cerámicos
Moldeo plástico

RESUMEN

En el presente trabajo, se elaboraron ladrillos a una escala real 1:1 para la construcción de viviendas. Para la preparación de las mezclas se utilizaron las materias primas como, arcilla, arena y vidrio obtenido del reciclaje de envases de cerveza color marrón aplicando el método de moldeo plástico para la preparación de los semiproductos. Se ha establecido que la adición de arena que contiene una pequeña cantidad de montmorillonita a tal arcilla permitió realizar el moldeo plástico. La incorporación de vidrio en la arcilla permitió reducir

* *Corresponding author.*
E-mail address: MFloresN@iingen.unam.mx (M. Flores Nicolás).
https://doi.org/10.1016/j.bsecv.2024.06.003

sustancialmente el tiempo de sinterización de los ladrillos hasta 8 h y variar sus propiedades de resistencia. La sinterización se ha realizado a 800 °C en una atmósfera de aire. Los resultados de los análisis de difracción de rayos X (DRX), fluorescencia de rayos X (FRX) y de microscopia electrónica de barrido de emisión de campo (FESEM), y microanálisis EDS, han demostrado que las materias primas y los ladrillos cerámicos contienen cuarzo y feldespatos. La sinterización a baja temperatura ha hecho posible obtener ladrillos de construcción de alta calidad y resistencia de acuerdo con las normas.

Introduction

For many years, the manufacture of bricks has been a significant building material widely used around the world. Its production requires the firing of clay in a kiln at high temperature over 1000 °C. The high temperature kiln firing not only consumes significant amount of energy but releases large quantity of greenhouse gases [1,2]. The purpose of firing is to improve durability gaining process of the clay brick, and that is succeeded through sintering [3]. Sintering is the heat treatment process in which a powder or porous material, already formed into a required shape, is converted to a useful solid [4]. Clays have been a material of great importance in the manufacture of ceramics, they are made up of various clay minerals (hydrated silicates, with ions mainly Mg, Fe, K, and Na) and other minerals such as quartz, feldspars, carbonates, final products of the destruction (weathering) of rocks under the influence of a complex set of processes: mechanical (water, wind, glaciers), physical (heating, cooling), chemical (exposure to moisture, oxygen, and carbon dioxide), bacteriological (decomposition of organic impurities) [5–15]. Clays contain mainly clay minerals, which are small silicates with a hydrated layer and are part of the phyllosilicate family. The term phyllosilicate is called "physics" in an abbreviated way to the word and has no connotations of particle size [6,16,17]. Clay minerals refer to a group of hydrated aluminosilicates that predominate in the clay fraction (<2 μm) of soils, these minerals are similar in chemistry and structure [17]. Clay refers to a naturally occurring material composed primarily of fine-grained minerals whose plasticity index (PI) is equal to or higher than the ratio of the liquid limit divided by two (LL/2), so that a clay is plastic or highly plastic at those water contents located between the liquid (LL) and plastic limit (PL) [18]. A moderately or slightly clayey material is a naturally occurring material composed primarily or partially of fine-grained minerals, whose plasticity index (PI) value is between the liquid limit divided by three (LL/3) and the ratio of the liquid limit divided by two (LL/2), so that a clayey material is slightly or moderately plastic at those water contents located between the liquid limit (LL) and plastic limit (PL). Both clays and materials with lower plasticity will harden when dried or fired, being this effect more pronounced as the value plastic index to liquid limit (PI/LL) ratio increases [18].

Nowadays, environmental problems have been considered as a serious situation due to the increasing amount of industrial waste such as glass bottles. One technique used to reduce such wastes is by recycling [19,20]. Using waste glass in brick manufacturing is a good way to keep waste glass out of landfills because they protect natural resources from further depletion, reduce greenhouse gas emissions, and lead to a more sustainable environment [21]. Today, environmentally friendly material recycling and energy saving are very important research fields [22]. One of the most common issues for Mexico and other countries is saving on the energy and the used raw materials in the production of construction materials such as brick [3]. In southern Mexico, specifically in the state of Guerrero, the brick making is still an artisanal activity that traditionally has been modified very little, the semi-products are sintered with temperatures greater than 1000 °C for 24 h or more sintering time in artisan kilns with high-energy consumption, mainly wood as fuel [23]. The peculiar problems of energy saving and the rational management of nature are of importance, in the case of wood there is no reforestation process [24].

The main objective of this study was the production of low-temperature sintered ceramic building bricks from clay, glass waste and sand.

Table 1 – Proportions of mixes.

Mix ID	Content, wt.%			
	Clay	Glass	Sand	Σ
M1	85.7	9.5	4.8	100
M2	81.8	9.1	9.1	100

Experimental procedure

The raw materials used to make the bricks were clay, sand, and ground cullet that after mixing were sintering at 800 °C, for 8 h. The clay was collected from the town of Changata, and the sand from the deposits of the Balsas River in the town of Villa Nicolás Bravo. As well as the glass bottles, these localities belong to the municipality of Ajuchitlán del Progreso in the state of Guerrero, Mexico. The mixtures were prepared by the powder method (grinding process), and the particle size of the sand and glass was 120 mesh (125 μm). For the preparation of the bricks, two mixture compositions were used (denoted as M1 and M2). These are presented in Table 1.

To prepare bricks with mixture M1, 13.5 kg of clay, 1.5 kg of glass and 0.75 kg of sand were used, 5.4 l of water were added. Finally, for manufacture bricks with mixture M2, 13.5 kg of clay, 1.5 kg of glass and 1.5 kg of sand were used, 5.4 l of water were added. The preparation of the paste to the elaboration of the semi-products, a Blakeslee Mod. F30 mixer was used, capacity 28.39 l. The mixing time of the mixer was 14 min where after 7 min it was turned off to remove the material from the bottom for 10 min manually and then it was mixed with the mixer for 7 min with a mixing speed of 1725 RPM. The components were homogenized until reaching a dough consistency, the dimensions of the wooden molds were a length of 28.5 cm, a width of 14.5 cm, and a height of 7.5 cm, for the elaboration of the semi-products the plastic molding method was used subsequently they were dried at room temperature for 20 days.

The clay sample was characterized by thermogravimetric (TG) analysis using LINSEIS STA PT 1600 equipment. The 26.042 mg aliquot was measured using an alumina crucible and sweep ramp of 10 °C/min. The temperature range was 30–1000 °C.

To calibrate the thermogravimetric curves, monohydrate calcium oxalate ($CaC_2O_4 - H_2O$) was used because this substance presents three very well-defined mass losses in the analyzed range. The curves were smoothed using the Savitzky–Golay routine. The Savitzky–Golay method is a filter used for smoothing functions. It is based on the calculation of a local polynomial regression (of degree k), with at least k+1 equally spaced points, to determine the new value of each point by obtaining a smooth function of the input data. This approximation preserves the characteristics of the initial distribution such as the relative maximums and minimums or the width of the peaks [25].

The whole-rock samples were ground to powder (finer than 75 μm) using a mortar and pestle. The powdered samples were mounted into back side aluminium sample holders. For clay separation, samples were gently disaggregated to avoid artificial grain size reduction of rock components, then broken into small chips (≈1 mm) using a porcelain crusher and dispersed in deionized water. Clay size fraction (<2 μm) was separated in distilled water according to Stokes' law using the most unaggressive method. Air-dried oriented preparations were obtained from the <2 μm fractions by pipetting some drops of the suspensions onto a glass slide and then drying at 30 °C for a few hours [26]. Ethylenglycol solvation of the slides was achieved by exposing them to ethylenglycol vapour at 70 °C for 24 h.

The whole-rock and clay fraction measurements were made using an EMPYREAN XRD diffractometer operating with an accelerating voltage of 45 kV and a filament current of 40 mA, using CuK_α radiation, nickel filter and PIXcel 3D detector. All samples were measured with a step size of 0.04° (2theta) and 40 s scan step time. Clay samples were examined by XRD in the air-dried form (AD), saturated with ethylene glycol (EG) and after heating (550 °C). The preparations were measured over a 2θ angle range of 2–80°.

The quantification was obtained using the RIR (reference intensity ratio [27]; and Rietveld [28]) methods, implemented in the HIGHScore v4.5 software and using the ICDD (International Center for Diffraction Data) and ICSD (Inorganic Crystal Structure Database). The refined specimen-dependent parameters were the zero error, displacement error, polynomial fitting for the background with six coefficients, cell parameters, and atomic coordinates. The quality of fitting by the

Table 2 – Heating cycle.

Time (min)	Temperature (°C)
$t_{01} = 30$	$C_{01} = 0$
$t_{02} = 10$	$C_{02} = 300$
$t_{03} = 20$	$C_{03} = 300$
$t_{04} = 10$	$C_{04} = 500$
$t_{05} = 30$	$C_{05} = 500$
$t_{06} = 10$	$C_{06} = 800$
$t_{07} = 480$	$C_{07} = 800$
$t_{08} = -121$	$C_{08} = 25$

Rietveld method has been controlled by the GOF index (goodness of fit) with values always less than 1.5. Based on the measurement of NIST standards, a maximum error of 10% is estimated in the quantitative analysis.

For X-ray fluorescence analysis of the raw materials a WD-FRX RIGAKU PRIMUS II sequential spectrometer equipped with rhodium (Rh) tube to be driven up to a maximum power of 4000 W and handling detection limits down to 1 μg/g was used. Microanalysis system with spot beam of 500 μm diameter (0.5 mm). The plasticity index was determined by the Atterberg method [29–31].

The YR series muffle was used for the sintering of the semi-products. Table 2 shows the values used to reach the temperature ramp of 800 °C for 8 h, the average heating rate is 10 °C/min, where t_{01}–t_{07} is the ramp time increment and C_{01}–C_{07} is the temperature increment value. The value of $t_{08} = -121$ which means the end of the program, out-put power off and C_{08} is the cooling of the furnace to an average ambient temperature of 25 °C.

Ceramic micrographs were analyzed by field emission scanning electron microscopy (FESEM) and EDS microanalysis, Schottky FESEM unit, model JEOL 7600F. For the FESEM investigation, the samples were prepared with the following dimensions 5 mm × 5 mm × 1 mm. The specimens were not plated with gold, the surfaces were analyzed directly.

The moisture of the specimens made with the M1 and M2 mixtures was calculated with the loss of moisture of the known mass after kiln drying at a temperature of 105 °C to constant weight. The apparent density ρ_b, of the ceramic samples M1 and M2 were evaluated as the weight/volume ratio of parallelepiped samples of known dimensions. The true density ρ_s, was calculated by the helium gas pycnometry method using a micromeritics brand displacement pycnometer, model AccuPyc II 1340 [32,33]. From the apparent and true densities, the total porosity ($Ø_T$) of the ceramic bricks was calculated as:

$$Ø_T = \left[1 - \frac{\rho_b}{\rho_s}\right] \times 100\% \quad (1)$$

Ten measurements were made to analyze the actual density and porosity of the specimens at the same time.

The shrinkage of the specimens was determined in two stages: drying shrinkage of the semi-product (Σ_1%) and shrinkage after sintering (Σ_2%) [34]. The total shrinkage was calculated by the formula:

$$\Sigma_T\,\% = \Sigma_1 + \Sigma_2 \quad (2)$$

Please cite this article in press as: M. Flores Nicolás et al., Low-temperature sintering of ceramic bricks from clay, waste glass and sand, Bol. Soc. Esp. Cerám. Vidr. (2024), https://doi.org/10.1016/j.bsecv.2024.06.003

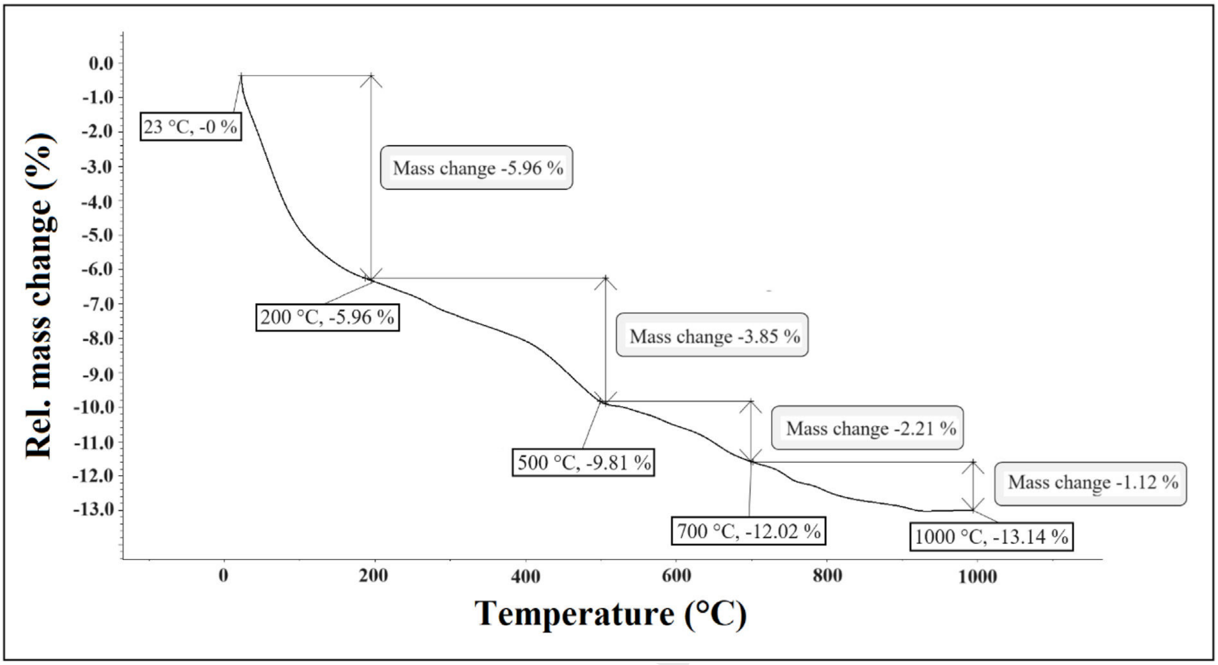

Fig. 1 – TG curve of clay sample.

$$\Sigma_1\,\% = 100 - \left[\frac{l_1 - l_0}{l_0}\right] \times 100 \quad (3)$$

$$\Sigma_2\,\% = 100 - \left[\frac{l_2 - l_1}{l_1}\right] \times 100 \quad (4)$$

where Σ_1 is the contraction during the drying process of the semi-products, Σ_2 is the contraction during sintering process, Σ_T is the total shrinkage of the sample.

Mechanical testing of the bricks was performed on a 2500 kN load frame, model 312.31, serial 1088. The compressive strength of the bricks was tested with a load applied at a speed of 156.91 kN/min (16 ton/min) based on the Mexican standard NMX-C-404-ONNCCE [35]. The compressive strength was calculated using the formula:

$$f_p = P/A\,(\mathrm{MPa}) \quad (5)$$

where f_p is the compressive strength (MPa), P is the maximum load (N), indicated by the testing machine, and A is the average of the areas of the upper and lower bearing surfaces of the specimen (mm^2).

In the study of the flexural strength, the brick was subjected to a point load with a speed of 8.89 kN/min (0.91 ton/min) in the center of the piece, recording the failure to breakage, these tests were carried out considering the standard norm ASTM C1161-02c [36]. The flexural strength was calculated by the formula:

$$R_{flex} = 3Wl/2bd^2\,(\mathrm{MPa}) \quad (6)$$

where R_{flex} is the flexural strength, W is the maximum load indicated by the machine test (N), l is the length of the support section (mm), b and d are the width and thickness of the specimen (mm) [36].

Results and discussion

Characterization of raw materials

Thermogravimetric analysis

Thermogravimetric analysis (TG) shows (Fig. 1) three main steps of mass loss. The mass loss below 500 °C measured constitutional waters and organic matter in the clay material. A value of 9.81% (5.96 + 3.85) ± 0.30% was obtained. Mass loss is much lower from 500 °C to 700 °C (2.21 ± 0.30%). The lowest mass loss is at high temperatures (700–1000 °C) with a value of 1.12 ± 0.30%). The values of mass loss are low because the proportion of clay minerals in the sample is also low (%). The most abundant minerals in the sample are quartz (29.20%) and feldspars (41.20%), anhydrous primary silicates that decompose at higher temperatures.

In Fig. 2, according to the first derivate of TG analysis (DTG), the presence of three clays was confirmed: kaolinite, illite, and smectite. For kaolinite in the temperature range 50–400 °C the first peak at 48.50 °C due to loss of adsorbed water, for the range 400–750 °C the second peak at 565.80 °C due to dehydroxylation of kaolinite, the third peak at 941.60 °C due to phase transition [37,38] to crystalline phases. In illite clay, the first peak at 268.30 °C end of the escape of adsorbed water and interlayer water, and the second peak (not well defined) at 452.60–565.80 °C belongs probably to dehydroxylation of illite [38–40]. Above 900 °C, the destruction of the crystalline lattice of this mineral occurs [40].

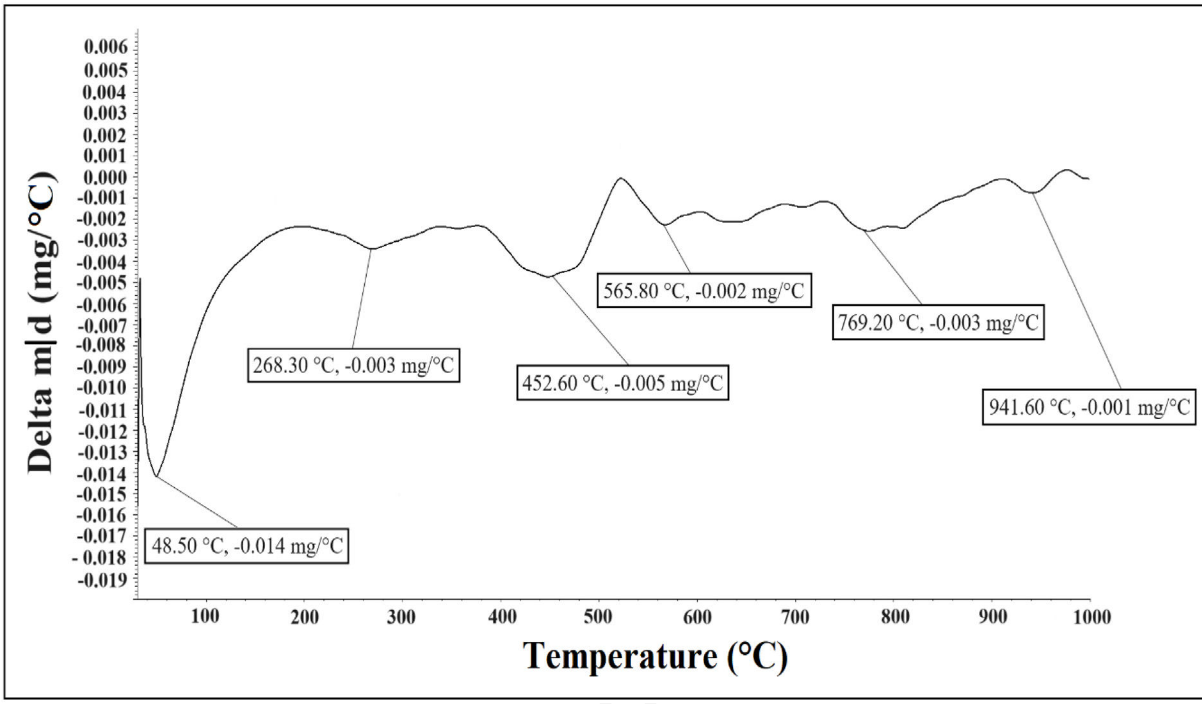

Fig. 2 – DTG curve of clay sample.

For smectite clay the first peak at 268.30 °C due to dehydration, for the second peak at 769.20 °C due to dehydroxylation and formation of amorphous phase. Above 900 °C, the decomposition of this mineral occurs [41].

X-ray diffraction of raw materials

Table 3 and Fig. 3 show the quantitative results of the analysis obtained by X-ray diffraction technique (XRD) of the raw materials by Rietveld method [28]: clay, glass and sand, it was observed that the composition of the main crystalline phases of the clay used that predominate the most are plagioclase (31.00%), quartz (29.20%) and sanidine (10.20%). The clay itself is a mixture of kaolinite (10.10%), illite (12.30%) and smectite (7.20%) (see Table 3 and Fig. 3a). The content of phyllosilicates did not exceed 29.60% among them, but a negligible amount of smectite (7.20%) is present. Fig. 3b shows the X-ray diffraction pattern of the glass used in the preparation of the mixtures, which presents a halo due to its amorphous structure. In the sand used, the crystalline phases are plagioclase (33.40%) and quartz (26.70%), which constitute the bulk of the material. However, phyllosilicates are also present in the sand (see Table 3 and Fig. 3c), with a content of 13.80% and in smaller amounts are found the crystalline phases of sanidine (15.40%), enstatite (9.00%) and hematite with 1.80%. The clay and sand samples analyzed for this investigation are quite similar. This mineralogical composition of the components corresponds to the early fracture stages of volcanic rocks [42].

Fig. 4 shows the main mineralogical components characterized by the X-ray diffraction technique in the clay fraction, the main phases identified were smectite, mica–illite and kaolinite. The presence of the smectite in the samples was confirmed by a very strong reflection (d_{001}) approximately at 2θ angle of 6° in the condition with untreated (oriented) peaks 13.16 Å,

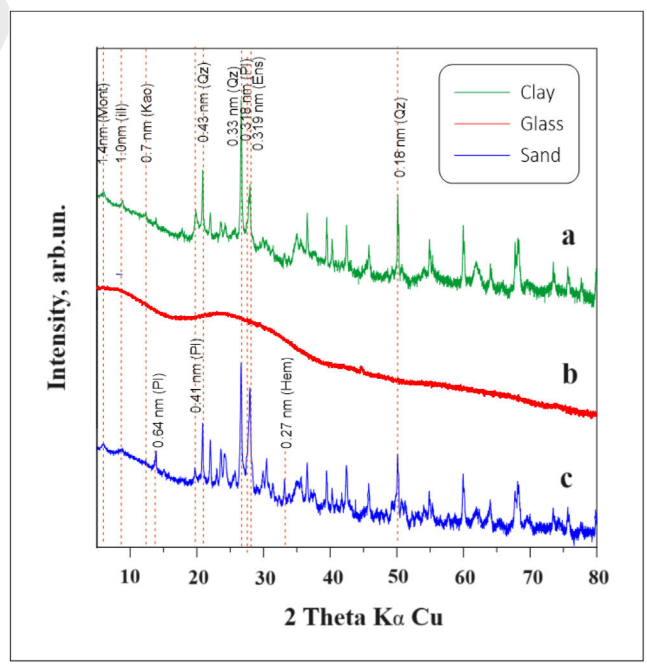

Fig. 3 – X-ray diffraction patterns of raw materials. Pl: plagioclase; ill: illite; Mont: smectite type montmorillonite; Qz: quartz; Kao: kaolinite; Ens: enstatite; Hem: hematite.

the smectite changed approximately at 2θ angle of 5.2° in the sample with ethylene glycol (glycolated) 16.93 Å and collapsed to 9.84 Å heated to 550 °C. For the mica–illite with untreated (oriented) peaks was identified at peak 10.30 Å, peaked with ethylene glycol (glycolated) 9.89 Å and heated at 550 °C, 9.84 Å.

Table 3 – Mineralogical composition (%) of the used components.

Group	Phase composition	Raw materials		
		Clay	Glass	Sand
	Quartz	29.20	–	26.70
Silicates	Plagioclase	31.00	–	33.40
	Sanidine	10.20	–	15.40
	Enstatite	–	–	9.00
Oxides	Hematite	–	–	1.80
	Kaolinite (structure 1:1)	10.10	–	4.20
Phyllosilicates	Smectite (structure 2:1)	7.20	–	2.80
	Illite (structure 2:1)	12.30	–	6.80
	Amorphous	–	100.00	–
	Total	100.00	100.00	100.00
	Σ phyllosilicates*	29.60		13.80

* This column is the sum of kaolinite, smectite and illite.

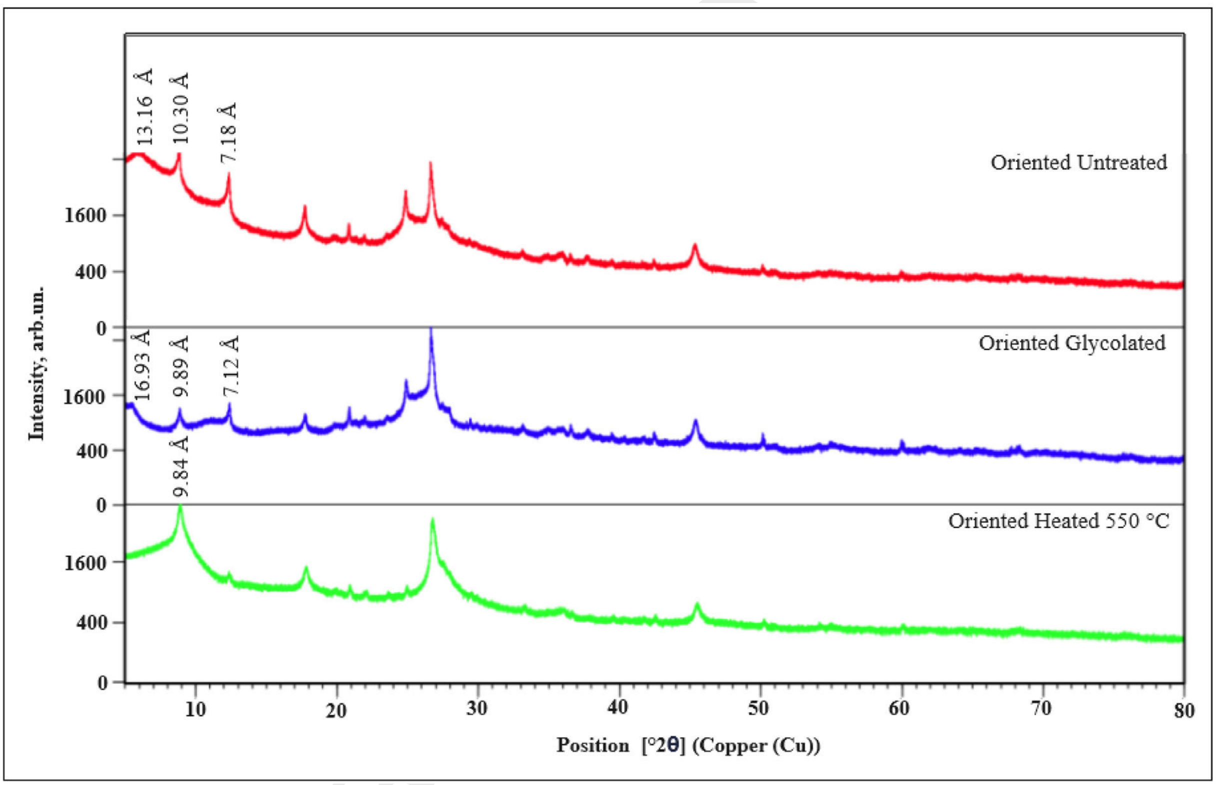

Fig. 4 – X-ray diffraction patterns of the oriented, glycolated, and heated clay fraction at 550 °C.

For its part, the kaolinite has similar peaks without treatment (oriented) and peaks with ethylene glycol (glycolated) at 7.18, 7.12 Å and collapsed completely when heated to 550 °C.

X-ray fluorescence analysis

Table 4 shows the chemical composition of the results obtained from the X-ray fluorescence analysis (XRF) of the raw materials. The main predominant chemical components of the clay were SiO_2 (61.42%), Al_2O_3 (17.54%) and Fe_2O_3 (6.35%), being the components with the lowest content TiO_2 (1.01%), MnO (0.09%) and P_2O_5 (0.05%). In the sand used, the chemical composition with the highest content was SiO_2 (67.69%), Al_2O_3 (14.69%) and Fe_2O_3 (4.54%), and in lower concentrations TiO_2 (0.79%), P_2O_5 (0.17%) and MnO (0.06%). In both samples, a high proportion of quartz stands out. The aluminum contents are related to the presence of anhydrous aluminosilicates (feldspars) and hydrated aluminosilicates (clay minerals). Calcium and sodium are found mainly in the structure of plagioclases (andesite), and potassium in sanidine and illite. Iron in the sand sample is associated with pyroxene-type mafic minerals (enstatite) and hematite. Enstatite also contains magnesium. For the clay sample, no iron or magnesium-rich minerals are found in XRD analysis, so these elements are contained probably in non-crystalline phases. In the case of glass, the main highest concentrations were SiO_2 (73.07%), CaO (13.03%) and Na_2O (9.71%). At

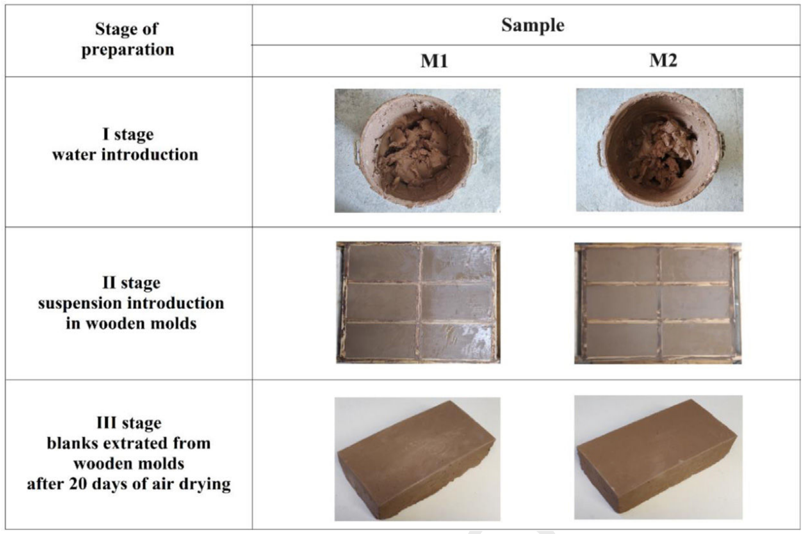

Fig. 5 – Different stages of preparation of semi-products.

Table 4 – The chemical composition (%) of raw materials analyzed by XRF.

Composition	Raw materials		
	Clay	Sand	Glass
SiO_2	61.42	67.69	73.07
Fe_2O_3	6.35	4.54	1.03
Al_2O_3	17.54	14.69	1.71
K_2O	2.18	2.81	0.93
CaO	1.74	1.30	13.03
Na_2O	1.11	4.08	9.71
TiO_2	1.01	0.79	0.13
P_2O_5	0.05	0.17	0.02
MgO	1.34	1.44	0.14
MnO	0.09	0.06	0.01
SO_3	–	–	0.08
PxC*	7.17	2.43	0.16

* PxC is the loss on calcination (PxC) and was determined with 1 g of ground sample powder calcined at 950 °C for 1 h and subsequently determining the mass loss by weighing. There is a good correlation between these values and the clay content of the sand and clay samples obtained by X-ray diffraction.

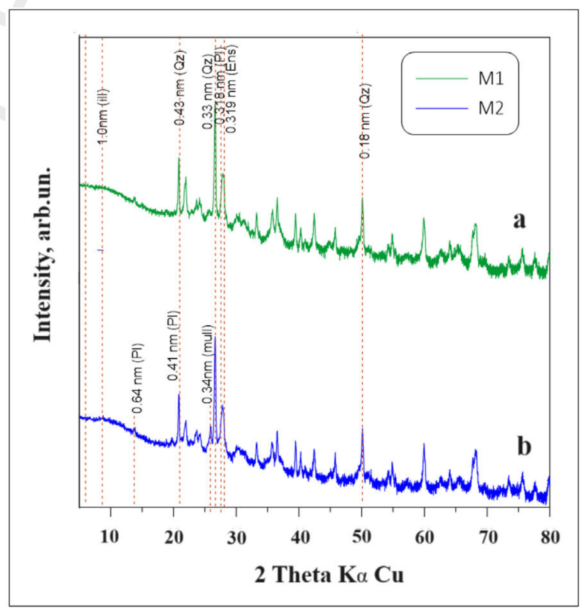

Fig. 6 – XRD patterns of the bricks made from the mixtures M1 and M2. $T_{sint.}$: 800 °C; $t_{sint.}$: 8 h; Pl: plagioclase; ill: illite; Qz: quartz; Kao: kaolinite; Ens: enstatite; Mull: mullite.

lower concentrations were SO_3 (0.08%), P_2O_5 (0.02%) and MnO (0.01%).

There is a very good agreement between the phase data obtained by X-ray diffraction and the X-ray fluorescence data. The theoretical composition of the sample has been recalculated based on the quantitative analysis of phases obtained by XRD and very good agreement (maximum error 8%) was obtained for all phases in both samples except for iron and magnesium, which in the clay sample appear to be in poorly crystalline phases not identified by XRD.

Plasticity

According to the results obtained by the Atterberg method, the clayey soil used showed a plasticity coefficient of 12.60. It was classified as low plasticity clay (CL) according to ASTM D2487 [43–45].

Characteristics of the molding preparation

For the preparation of the semi-products, the plastic molding method was used, 5.4 l of water were added to the mixtures and the wooden molds were filled with paste, then the samples were dried at room temperature for 20 days (see Fig. 5).

Characterization of ceramic bricks materials

X-ray diffraction

Fig. 6 shows the XRD patterns of the bricks made from the mixtures M1 and M2. The results obtained from the X-ray diffraction of the bricks made with the mixture M1 showed

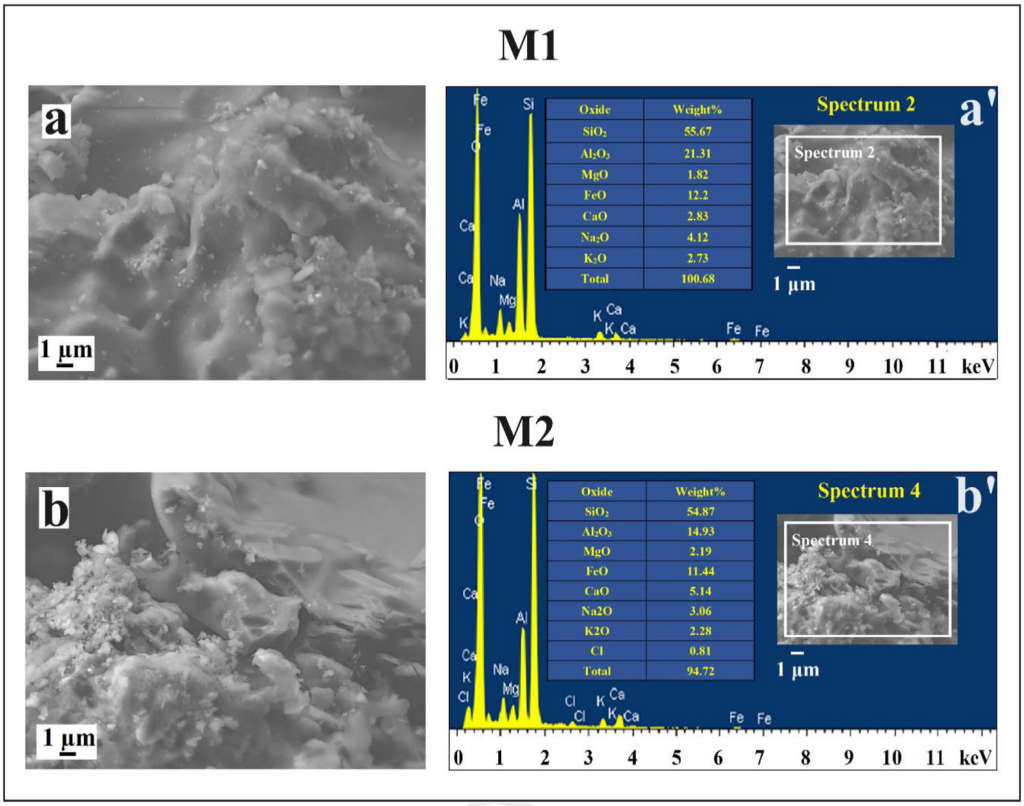

Fig. 7 – Micrographs of fractures of bricks made with mixtures M1 and M2 (a and b) and contents of elements at different places of the ceramics indicated in (a′, b′). $T_{sint.}$: 800 °C, $t_{sint.}$: 8 h.

that the composition of the main crystalline phases identified in the respective diffractograms are andesine (52.80%), quartz (43.10%), illite–smectite (2.60%) and enstatite, ferroan (1.40%) (see Fig. 6a). The bricks made with the mixture M2, its main crystalline phases are andesine (61.60%), quartz (33.30%), illite–smectite (4.2), enstatite, ferroan (0.50%) and mulite (0.30%) (see Fig. 6b).

FESEM analysis

In Fig. 7, the micrographs obtained by FESEM are presented, it was observed in Fig. 7a and b, the ceramic material consists of large particles embedded in a finer-grained material. In all ceramic materials, pores are present. EDS results (Fig. 7a′, b′) showed similar percentages SiO_2 (55.67–54.87%), Al_2O_3 (21.31–14.93%) and FeO (12.2–11.44%) in the bricks made with mixtures M1 and M2, record solidified melt areas of different sizes, which bind grains of more refractory material. While other oxides, as CaO (2.83–5.14%), Na_2O (4.12–3.06%), K_2O (2.73–2.28%), MgO (1.82–2.19%) and Cl are less represented. The chlorine (Cl) was found in the bricks of the mixture M2 in less percentage, i.e. approximately 0.81% (see Fig. 7b′). The presence of Cl in the analyses implies that in the composition of the ceramic body there are not only oxides, but also chlorides, given the heterogeneous distribution of the materials that make up the ceramic body. The EDS analysis showed that both bricks M1 and M2 contain the main oxides.

Moisture, density and porosity of ceramic bricks

Table 5 shows that the values of apparent and true density of the specimens made with the M1 and M2 mixtures studied do not differ significantly from the ceramic. This is due to the fact that the mineralogical composition of clay and sand are similar to each other, plagioclase, quartz and phyllosilicates present in clay and sand, as well as glass are melting agents. In the case of moisture, the bricks made with the M2 mixture have higher moisture of content of 1.29% compared to the bricks made with the M1 mixture that contain lower moisture of 0.06%, to explain this result the bricks made with the M2 mixture contain higher amount of sand and therefore have higher porosity than the bricks made with the M1 mixture (see Table 5).

Shrinkage

Brick shrinkage occurs as a result of the evaporation of water from during both drying and firing processes of the semi-products [34,46]. Fig. 8 shows the percentage of shrinkage of the ceramic bricks made with mixtures M1 and M2. Column 1 represents the drying shrinkage of the specimens (20 days), column 2 the shrinkage when the semi-products were sintered at a temperature of 800 °C for 8 h and column 3 the total shrinkage of the bricks. As can be seen, the total shrinkage of the bricks made with mixture M2 was 10.55%, the shrinkage of these bricks is similar to the bricks made with mix M1, whose total shrinkage was 10.19%. This is because that both samples

Table 5 – Ceramic bricks properties.

Mix ID	Moisture %	Apparent density g/cm^3	Real density gas pycnometry (helium) g/cm^3	Total porosity ($\varnothing_T$), %
M1	0.06	1.79	2.55	29.80
M2	1.29	1.90	2.71	29.89

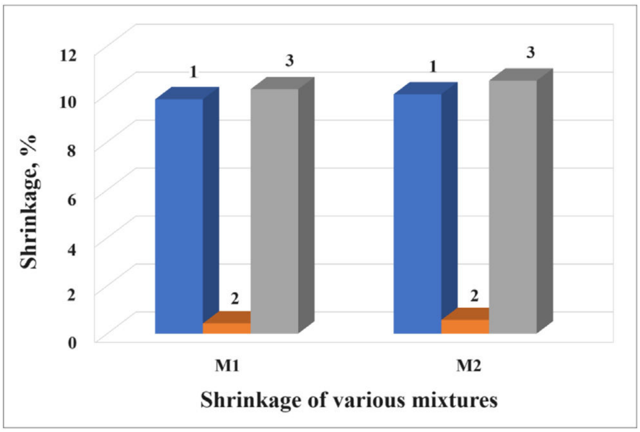

Fig. 8 – Shrinkage mechanism analysis of bricks made with mixtures M1 and M2. For shrinkage in the sintering regime $T_{sint.}$: 800 °C, $t_{sint.}$: 8 h.

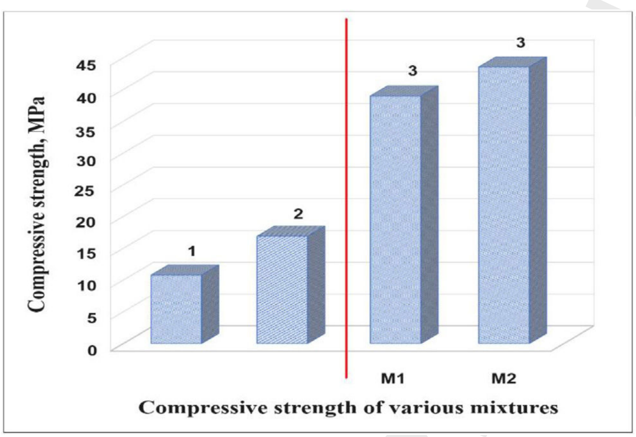

Fig. 9 – Column 1 corresponds to Mexican standard NMX-C-404-ONNCCE, column 2 corresponds to the studies of the mechanical properties of the handmade bricks in the State of Guerrero, Mexico and column 3 corresponds to the experimental data of the bricks made with mixtures M1 and M2.

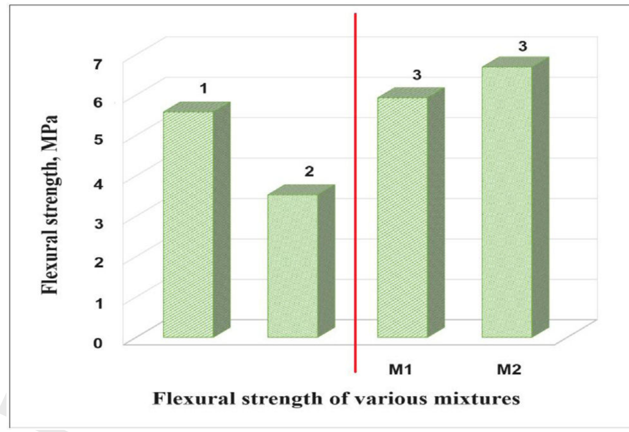

Fig. 10 – Column 1 corresponds to the ASTM C1161-02c, column 2 corresponds to the studies of the mechanical properties of the handmade bricks in the State of Guerrero, Mexico and column 3 corresponds to the experimental data of the bricks made with mixtures M1 and M2.

have similar concentration of phyllosilicates and M1 sample has more while its shrinkage is less.

Mechanical properties of ceramics

Compressive strength. The compressive strength is highly important, because the function of the ceramic brick is basically to support compressive stress. Fig. 9 shows the results of the compressive strength of the bricks made with mixtures M1 and M2 (see Fig. 9, column 3). Table 6 shows the minimum compressive strength according to different standards of different countries based on bricks classification [47–58]. The results in Fig. 9 show that the bricks made with mixture M1 presented lower compressive strength of 38.98 MPa by adding 4.8 wt.% sand of sand and 9.5 wt.% of glass (see Table 1) compared to the bricks made with mixture M2 presented the maximum compressive strength of 43.55 MPa by adding 9.1 wt.% sand and 9.1 wt.% glass (see Table 1). To explain this result, the composition of the clay and sand used must be taken into account, which contains a large amount of feldspars and quartz and a smaller amount of clays. The ceramic bricks obtained from mixtures M1 and M2 have good compressive strength properties due to the devitrification of the glass from a solid phase to a liquid phase. Filling the open pores, i.e. it binds all the refractory particles of quartz and feldspar together. The compressive strength of the bricks made with the M1 and M2 mixtures are higher than the minimum compressive strength specification of 11 MPa required by the Mexican standard NMX-C-404-ONNCCE (see Fig. 9, column 1) and by the standards presented in Table No. 6 [47–60]. It was also compared with the studies of the mechanical properties of the handmade brick produced in the state of Guerrero, Mexico (see Fig. 9, column 2), whose strengths are lower in compared with the compressive strengths of the bricks made with the M1 and M2 mixtures.

Flexural strength. Fig. 10 shows the results of the flexural strength of the bricks prepared with M1 and M2 mixtures (see Fig. 10, column 3). The results of flexural strength of the bricks prepared with the M1 mixture were 5.93 MPa and for the bricks

Please cite this article in press as: M. Flores Nicolás et al., Low-temperature sintering of ceramic bricks from clay, waste glass and sand, Bol. Soc. Esp. Cerám. Vidr. (2024), https://doi.org/10.1016/j.bsecv.2024.06.003

Table 6 – Standard minimum compressive strength requirement as per different standards.

International standard	Designation	Brick classification	Minimun compressive strength (MPa)
Building bricks	ASTM C62-13a, 2013 [48]	Severe weathering	20.7
		Moderate weathering	17.2
		Negligible weathering	10.3
Solid Masonry Unit	ASTM C126-16, 2011 [49]	Vertical coring	20.7
		Horizontal coring	13.8
Facing bricks	ASTM 216-16, 2013 [50]	Severe weathering	20.7
		Moderate weathering	17.2
China National Standard	CNS382-R2002, 2007 [51]	First degree	14.71
		Second degree	9.81
		Third degree	7.35
		Pavement bricks	49.03
Brazilian Standard	NBR 6064 (ABNT 1983a) [52]	Clay bricks	1.5
Common burnt clay bricks	IS 1077, 2007 [53]	Burnt clay bricks	3.5–35
Hollow clay bricks	IS 3952, 2006 [54]	Hollow bricks	3.5
Burnt clay fly ash bricks	IS 13757, 1993 [55]	Fly ash bricks	3.5–30
Calcium silicate bricks	IS 4139, 2004 [56]	Calcium silicate bricks	7.5–20
Pulverized fuel ash lime bricks	IS 12894, 2002 [57]	Fuel ash lime brick	3.5–35
Hollow concrete blocks	IS 2185-1, 2005 [58]	Grade A	3.5–15
		Grade B	3.5–5
		Grade C	4–5

made with the M2 mixtures 6.69 MPa, exceeding the specifications of the ASTM C1161-02c standard (see Fig. 10, column 1) [36] and the studies of the mechanical properties of the handmade brick produced in the state of Guerrero (see Fig. 10, column 2).

Conclusions

According to the results, obtained in this research, it was verified that the selected raw material, i.e., clay, belongs to a siliceous clay with small amounts of kaolinite and montmorillonite. The sand that was added to the clay also contains small amounts of montmorillonite and kaolinite. It should be noted that siliceous clays are used to produce refractory ceramics by a process that is fundamentally different from the usual process of producing bricks from plastic clays. Thus, as a result of this research, the approach we have developed for low-temperature sintering of siliceous clays was added ground glass for the production of building ceramics by plastic molding, thus solving the problem of energy saving as well as the problem of glass waste disposal (ecological problem).

The physical and mechanical properties of the ceramic brick with the addition of waste glass and sand were studied. The results showed that the compressive strength of the bricks made with the M2 mixture increased with the addition of 9.1 wt.% sand and 9.1 wt.% glass. The compressive strength of the bricks made with the M1 and M2 mixtures are higher than the minimum compressive strength specification of 11 MPa required by the Mexican standard NMX-C-404-ONNCCE.

The values of apparent and true density of the specimens made with the M1 and M2 mixtures studied do not differ significantly from the ceramic. This is due to the fact that the mineralogical composition of clay and sand are similar to each other, feldspars, quartz and phyllosilicates present in clay and sand, as well as glass are melting agents. In addition, it was possible to reduce the sintering temperature and time in an air atmosphere to 800 °C for 8 h. The simultaneous improvement of the mechanical properties allows the application of these ceramic materials in load-bearing masonry walls for the design of sustainable buildings. The south Mexico is located in a highly seismic zone of the country. For these reasons, this material has relevant importance.

Acknowledgements

The authors acknowledge the support provided by the CONAHCYT National Laboratories Projects and University Laboratory of Electron Microscopy “LUME”. We acknowledge Rufino Lozano from the Instituto de Geología and LANGEM (UNAM), for the X-ray fluorescence analyses. The authors would also like to thank Jorge René Alcalá Martínez of the Soil Physics Laboratory of LANGEM (National Laboratory of Geochemistry and Mineralogy) for porosity determination.

REFERENCES

[1] L. Zhang, Production of bricks from waste materials – a review, Constr. Build. Mater. 47 (2013) 643–655, http://dx.doi.org/10.1016/j.conbuildmat.2013.05.043.

[2] G.S. dos Reis, B.G. Cazacliu, A. Cothenet, P. Poullain, M. Wilhelm, C.H. Sampaio, E.C. Lima, W. Ambros, J.M. Torrenti, Fabrication, microstructure, and properties of fired clay bricks using construction and demolition waste sludge as the main additive, J. Clean. Prod. 258 (2020) 120733, http://dx.doi.org/10.1016/j.jclepro.2020.120733.

[3] G. Görhan, O. Şimşek, Porous clay bricks manufactured with rice husks, Constr. Build. Mater. 40 (2013) 390–396, http://dx.doi.org/10.1016/j.conbuildmat.2012.09.110.

[4] M.N. Rahaman, Sintering of Ceramics, CRC Press, 2007.

[5] S. Wang, L. Gainey, D. Baxter, X. Wang, I.D.R. Mackinnon, Y. Xi, Thermal behaviours of clay mixtures during brick firing: a combined study of in-situ XRD, TGA and thermal

dilatometry, Constr. Build. Mater. 299 (2021) 124319, http://dx.doi.org/10.1016/j.conbuildmat.2021.124319.

[6] L.A. Díaz Rodríguez, R. Torrecillas, Arcillas cerámicas: una revisión de sus distintos tipos, significados y aplicaciones, Bol. Soc. Esp. Ceram. Vidr. 41 (5) (2002) 459–470, http://dx.doi.org/10.3989/cyv.2002.v41.i5.665.

[7] N.F. Solodkiv, V.V. Viktorov, E.N. Solodkiy, M.N. Solodkaya, V.M. Pogrebenkov, Mineral Resource Base of the Urals for the Ceramic, Refractory and Glass Industries, 2018, https://www.geokniga.org/books/15561 (in Russian).

[8] H.H. Murray, Developments in clay science, in: H.H. Murray (Ed.), Applied Clay Mineralogy. Occurrences, Processing and Application of Kaolins, Bentonites, Palygorskite–Sepiolite, and Common Clays, Elsevier Science, Amsterdam, 2007, pp. 644–645.

[9] S.W. Bailey, Summary of recommendations of AIPEA nomenclature committee on clay minerals, Am. Miner. 65 (1–2) (1980) 1–7, http://dx.doi.org/10.1180/claymin.1980.015.1.07.

[10] R.T. Martin, S.W. Bailey, D.D. Eberl, D.S. Fanning, S. Guggenheim, H. Kodama, F.J. Wicks, Report of the clay minerals society nomenclature committee: revised classification of clay materials, Clay Clay Min. 39 (3) (1991) 333–335, http://dx.doi.org/10.1346/CCMN.1991.0390315.

[11] S. Guggenheim, J.M. Adams, D.C. Bain, F. Bergaya, M.F. Brigatti, V.A. Drits, H. Stanjek, Summary of recommendations of nomenclature committees relevant to clay mineralogy: report of the association Internationale Pour L'etude des Argiles (AIPEA) Nomenclature Committee for 2006, Clay Clay Min. 54 (6) (2006) 761–772, http://dx.doi.org/10.1346/CCMN.2006.0540610.

[12] F. Bergaya, G. Lagaly, Handbook of clay science, in: F. Bergaya, B.K.G. Theng, B. Lagaly (Eds.), Developments in Clay Science, Vol. 1, Elsevier, 2006, pp. 1–18, http://dx.doi.org/10.1016/S1572-4352(05)01001-9.

[13] M.F. Brigatti, D. Malferrari, A. Laurora, C. Elmi, Structure and mineralogy of layer silicates: recent perspectives and new trends, in: M.F. Brigatti, A. Mottana (Eds.), Layered Mineral Structures and their Application in Advanced Technologies, 2011, pp. 1–71, http://dx.doi.org/10.1180/EMU-notes.11.

[14] G. Brown, Crystal structures of clay minerals and related phyllosilicates, Philos. Trans. R. Soc. Lond. Ser. A, Math. Phys. Sci. 311 (1517) (1984) 221–240, http://dx.doi.org/10.1098/rsta.1984.0025.

[15] R.E. Grim, Relation of the composition to the properties of clays, J. Am. Ceram. Soc. 22 (1–12) (1939) 141–151, http://dx.doi.org/10.1111/j.1151-2916.1939.tb19440.x.

[16] C.E. Weaver, Clays, Muds, and Shales. Developments in Sedimentology, Vol. 44, 1st edition, Elsevier, 1989.

[17] R.E. Grim, Clay Mineralogy, 2nd edition, McGraw-Hill, 1968.

[18] J.M. Moreno-Maroto, J.J. Alonso-Azcárate, What is clay? A new definition of "clay" based on plasticity and its impact on the most widespread soil classification systems, Appl. Clay Sci. 161 (2018) 57–63, http://dx.doi.org/10.1016/j.clay.2018.04.011.

[19] V.Y. Tam, V.C.M. Tam, A review on the viable technology for construction waste recycling, Resour. Conserv. Recycl. 47 (3) (2006) 209–221, http://dx.doi.org/10.1016/j.resconrec.2005.12.002.

[20] V. Loryuenyong, T. Panyachai, K. Kaewsimork, C. Siritai, Effects of recycled glass substitution on the physical and mechanical properties of clay bricks, Waste Manage. 29 (10) (2009) 2717–2721, http://dx.doi.org/10.1016/j.wasman.2009.05.015.

[21] N. Sharma, P. Sharma, A.K. Parashar, Use of waste glass and demolished brick as coarse aggregate in production of sustainable concrete, Mater. Today Proc. 62 (2022) 4030–4035, http://dx.doi.org/10.1016/j.matpr.2022.04.602.

[22] I. Demir, Effect of organic residues addition on the technological properties of clay bricks, Waste Manage. 28 (3) (2008) 622–627, http://dx.doi.org/10.1016/j.wasman.2007.03.019.

[23] M. Flores Nicolás, M. Vlasova, P.A. Márquez Aguilar, M. Kakazey, M.M. Chávez Cano, R. Arroyo Matus, T. Pi Puig, Development of an energy-saving technology for sintering of bricks from high-siliceous clay by the plastic molding method, Constr. Build. Mater. 242 (2020) 118142, http://dx.doi.org/10.1016/j.conbuildmat.2020.118142.

[24] A.A. Shakir, A.A. Mohammed, Manufacturing of bricks in the past, in the present and in the future: a state of the art review, Int. J. Adv. Appl. Sci. 2 (3) (2013) 145–156.

[25] A. Savitzky, M.J. Golay, Smoothing and differentiation of data by simplified least squares procedures, Anal. Chem. 36 (8) (1964) 1627–1639, http://dx.doi.org/10.1021/ac60214a047.

[26] D. Moore, R.C. Reynolds Jr., X-ray Diffraction and the Identification and Analysis of Clay Minerals, 2nd edition, Oxford University, 1997.

[27] C. Hubbard, R. Snyder, RIR – measurement and use in quantitative XRD, Powder Diffr. 3 (2) (1988) 74–77.

[28] H.M. Rietveld, A profile refinement method for nuclear and magnetic structures, J. Appl. Cryst. 2 (2) (1969) 65–71, http://dx.doi.org/10.1107/S0021889869006558.

[29] ASTM D 4318-05, Standard Test Methods for Liquid Limit, Plastic Limit and Plasticity Index of Soils, ASTM International, West Conshohocken, PA, USA, 2005.

[30] E.J. Badillo, A.R. Rodrigues, Mecánica de Suelos, v.1. Fundamentos de la Mecánica de Suelos, LIMUSA, México, 2005.

[31] M. Mendoza, M. Orosco, Técnicas Alternativas para la determinación del Límite Líquido de Suelos, Instituto de Ingeniería de la UNAM, 2000.

[32] R. Burt, Soil Survey Laboratory Methods, Soil Survey Investigations Report No. 42 Version 4.4 Natural Resources Conservation Service, Ed. Rebecca Burt, United States Department of Agriculture, 2004.

[33] R.J.H.G. Clarke Topp, Methods of soil analysis, part 4 physical methods, in: J.H. Danes, G.C. Topp (Eds.), Number 5 in the Soil Science Society of America Book Series, Soil Science Society of America, Inc., Madison, WI, USA, 2002.

[34] ASTM C326-82, Standard Test Method for Drying and Firing Shrinkage of Ceramic Whitewares Clays, ASTM International, West Conshohocken, PA, 2002.

[35] Standard Specification for Building Brick. Norma Mexicana NMX-C404-ONNCCE-2012.

[36] ASTM C1161-02c e1, Standard Test Method for Flexural Strength of Advanced Ceramics at Ambient Temperature, ASTM International, West Conshohocken, PA, 2008.

[37] R.C. Mackenzie, S. Caillere, Thermal analysis DTA, TG, DTG, in: H. Van Olphen, J.J. Fripiat (Eds.), Data Handbook for Clay Materials and Other Non-metallic Minerals, Pergamon Press, Oxford, 1979, pp. 243–284.

[38] M. Földvari, Handbook of thermogravimetric system of minerals and its use in geological practice, in: Occasional Papers of the Geological Institute of Hungary, Vol. 213, 2011.

[39] P. Ptáček, D. Kubátová, J. Havlica, J. Brandštetr, F. Šoukal, T. Opravil, Isothermal kinetic analysis of the thermal decomposition of kaolinite: the thermogravimetric study, Thermochim. Acta 501 (2010) 24–29, http://dx.doi.org/10.1016/j.tca.2009.12.018.

[40] C.M. Earnest, Thermal analysis of selected illite and smectite clay minerals. Part I. Illite clay specimens, in: W. Smykatz-Kloss, S.S.J. Warne (Eds.), Thermal Analysis in the Geosciences. Lecture Notes in Earth Sciences, Vol. 38, Springer, Berlin, Heidelberg, 1991, http://dx.doi.org/10.1007/BFb0010271.

Please cite this article in press as: M. Flores Nicolás et al., Low-temperature sintering of ceramic bricks from clay, waste glass and sand, Bol. Soc. Esp. Cerám. Vidr. (2024), https://doi.org/10.1016/j.bsecv.2024.06.003

[41] C.M. Earnest, Thermal analysis of selected illite and smectite clay minerals. Part II. Smectite clay minerals, in: W. Smykatz-Kloss, S.S.J. Warne (Eds.), Thermal Analysis in the Geosciences. Lecture Notes in Earth Sciences, Vol. 38, Springer, Berlin, Heidelberg, 1991, http://dx.doi.org/10.1007/BFb0010272.

[42] R.L. Bates, Geology of the Industrial Rocks and Minerals, Harper and Brothers Publishers, New York, 1960.

[43] ASTM D2487, Standard Practice for Classification of Soils for Engineering Purposes (Unified Soil Classification System), ASTM International, West Conshohocken, PA, 2011.

[44] H. MolaAbasi, P. Kharazmi, A. Khajeh, M. Saberian, R.J. Chenari, M. Harandi, J. Li, Low plasticity clay stabilized with cement and zeolite: an experimental and environmental impact study, Resour. Conserv. Recycl. 184 (2022) 106408, http://dx.doi.org/10.1016/j.resconrec.2022.106408.

[45] A.F. Cabalar, M.H. Awraheem, M.M. Khalaf, Geotechnical properties of a low-plasticity clay with biopolymer, J. Mater. Civil Eng. 30 (8) (2018), http://dx.doi.org/10.1061/(ASCE)MT.1943-5533.000238, 04018170.

[46] M.W. Tjaronge, M.A. Caronge, Physico-mechanical and thermal performances of eco-friendly fired clay bricks incorporating palm oil fuel ash, Materials 17 (2021) 101130, http://dx.doi.org/10.1016/j.mtla.2021.101130.

[47] A.L. Murmu, A. Patel, Towards sustainable bricks production: an overview, Constr. Build. Mater. 165 (2018) 112–125, http://dx.doi.org/10.1016/j.conbuildmat.2018.01.038.

[48] ASTM-C62-13a, Standard Specification for Hollow Brick (Hollow Masonry Units Made from Clay or Shale), 2013.

[49] ASTM-C126-16, Standard Specification for Ceramic Glazed Structural Clay Facing Tile, Facing Brick, and Solid Masonry Units 1, 2011.

[50] ASTM-C216-16, Standard Specification for Hollow Brick (Hollow Masonry Units Made From Clay or Shale), 2013.

[51] CNS382-R2002, Building With Ordinary Brick, Natl. Stand. Repub. China, 2007.

[52] NBR-6064, Solid Ceramic Brick for Masonry – Verification of Compressive Strength – Test Method, Brazilian Assoc. Tech. Standards, Brazil, 1983.

[53] IS-1077, Common Burnt Clay Building Bricks – Specification, Bur. Indian Stand., 2007.

[54] IS-3952, Burnt Clay Hollow Bricks for Walls and Partitions – Specification, Bur. Indian Stand., 2006.

[55] IS-13757, Burnt Clay Fly Ash Building Bricks, Bur. Indian Stand., 1993.

[56] IS-4139, Calcium Silicate Bricks, Bur. Indian Stand., 2004.

[57] IS-12894, Pulverized Fuel Ash-Lime Bricks, Bur. Indian Stand., 2002.

[58] IS-2185-1, Concrete Masonry Units, Part 1: Hollow and Solid Concrete Blocks, Bur. Indian Stand., 2005.

Please cite this article in press as: M. Flores Nicolás et al., Low-temperature sintering of ceramic bricks from clay, waste glass and sand, Bol. Soc. Esp. Cerám. Vidr. (2024), https://doi.org/10.1016/j.bsecv.2024.06.003